HIGH RESOLUTION – HIGH FOCUSED SQUINT-MODE RADAR IMAGING USING THE FRACTIONAL CHIRP SCALING ALGORITHM

A. S. Amein, John J. Soraghan

The institute of communication and signal processing, University of Strathclyde, Scotland, UK

ABSTRACT

The fractional Fourier transform (FrFT), which is a generalized form of the well-known Fourier transform, has only recently started to appear in the field of signal processing. This has opened up the possibility of a new range of potentially promising and useful applications. In this paper we apply the new FrFT-based Chirp Scaling Algorithm (CSA) to a high resolution-high focused Synthetic Aperture Radar (SAR) imaging and compare its performance with the classical CSA based on the Fast Fourier Transform (FFT). Simulation results show that the FrFT-based CSA can offer significantly enhanced features compared to the classical FFT-based approach.

1. INTRODUCTION

The fractional Fourier transform (FrFT) was derived by Namias in the 80s as a new mathematical tool in order to deal with certain problems in quantum mechanics [1]. The first introduction to the application of FrFT in signal processing was published by Almeida [2]. A more recent introduction to the FrFTs and their applications is given in [3,16-17], which describe a number of promising research areas for further investigation including radar applications involving the use and detection of chirp signals, pattern recognition and Synthetic Aperture Radar (SAR) image processing.

Imaging radars typically provide a two-dimensional representation of scatterer in the illuminated volume with no resolution or positioning of scatterers in the third dimension. Generally, we speak of radar resolution in the range and cross-range or azimuth directions. The Chirp Scaling Algorithm (CSA) [4] is one of the most important and well-known radar imaging algorithms. It is attractive because of its excellent focusing ability and implementation simplicity.

Benefiting from the inherent structure of the FrFT for non-stationary digital signal processing and analysis, especially for chirped-type signals, a new version of the CSA based on the Fractional Fourier Transform (FrFT) was introduced in [5]. The new Fractional Chirp Scaling Algorithm (FrCSA) was shown to significantly outperform the conventional CSA in terms of resolution, SNR and sidelobe suppression.

In this paper, we use the FrCSA to obtain a high resolution – high focused SAR imaging and compare this result with that of the classical FFT-based CSA. The rest of this paper is organized as follows: Section 2 introduces the FrFT and its various mathematical properties. Section 3 presents the mathematical model for the FrCSA. This is followed by some simulation experiments described in Section 4. Finally, some concluding remarks and future work proposals are given in Section 5.

2. THE FRACTIONAL FOURIER TRANSFORM

As the classical Fourier transform (FT) corresponds to a rotation in the time-frequency plane over an angle $\alpha = \pi/2$, the FrFT can be considered as a generalized form that corresponds to a rotation over some arbitrary angle $\alpha = a\pi/2$ with $a \in \Re$.

The continuous 1-D FrFT is defined by means of the following transformation kernel [2]:

$$K_\alpha(t,u) = \begin{cases} \sqrt{\dfrac{1-j\cot\alpha}{2\pi}}\, e^{j\frac{t^2+u^2}{2}\cot\alpha - jut\csc\alpha} & \\ & if\ \alpha\ is\ not\ a\ multiple\ of\ \pi \\ \delta(t-u) & if\ \alpha\ is\ a\ multiple\ of\ 2\pi \\ \delta(t+u) & if\ \alpha+\pi\ is\ a\ muliple\ of\ 2\pi \end{cases} \quad (1)$$

Given that F is the Fourier transform operator and F_r^α is the fractional Fourier transform operator, then the fractional Fourier transform possesses the following important properties:

1) Zero rotation: $F_r^0 = I$

2) Consistency with Fourier transforms: $F_r^{\pi/2} = F$

3) Additivity of rotations: $F_r^\beta F_r^\alpha = F_r^{\alpha+\beta}$

4) 2π rotation: $F_r^{2\pi} = I$

5) Inverse FrFT: $F_r^{-1}(\alpha) = F_r(-\alpha)$

In addition, the FrFT kernel has the following properties, which will be of interest in this work:

1) $K_\alpha(t,u) = K_\alpha(u,t)$

1-4244-0469-X/06/$20.00

2) $\int_{-\infty}^{\infty} K_\alpha(t,u)K_\alpha^*(t,u')dt = \delta(u-u')$

3) $K_\alpha(-t,u) = K_\alpha(t,-u)$

4) $\int_{-\infty}^{\infty} K_\alpha(t,u)K_\beta(u,z)du = K_{\alpha+\beta}(t,z)$

5) $K_{-\alpha}(t,u) = K_\alpha^*(t,u)$, where * indicates the complex conjugate

Further properties of the FrFT and sample transforms of some common functions can be found in [2][3].

Formally, the fractional Fourier transform of an arbitrary function *x(t)*, with an angle α, is defined as:

$$X_\alpha(u) = \int_{-\infty}^{\infty} x(t)K_\alpha(t,u)dt$$

$$= \begin{cases} \sqrt{\dfrac{1-j\cot\alpha}{2\pi}}\, e^{j\frac{u^2}{2}\cot\alpha} \displaystyle\int_{-\infty}^{\infty} x(t) e^{j\frac{t^2}{2}\cot\alpha} e^{jut\csc\alpha} dt & \\ & if\ \alpha\ is\ not\ a\ multiple\ of\ \pi \\ x(t) & if\ \alpha\ is\ a\ multiple\ of\ 2\pi \\ x(-t) & if\ \alpha+\pi\ is\ a\ multiple\ of\ 2\pi \end{cases} \quad (2)$$

Equation (2) shows that for angles that are not multiples of π, the computation of the FrFT corresponds to the following steps:

1-A product by a chirp

2-A Fourier transform (scaled by *Csc(*α*)*)

3-Another product by a chirp

4-A product by a complex amplitude factor

In summary, the FrFT is a linear transform, continuous in the angle α, which satisfies the basic conditions for it to be meaningful as a rotation in the time-frequency plane.

3. FRACTIONAL CHIRP SCALING ALGORITHM

The conventional FFT-based CSA block diagram is illustrated in Figure 1, note that the algorithm uses FFTs and complex vector multiplications. This is the main reason for the CSA's accuracy and efficiency [4]. There are some important issues related to the CSA applicability and performance. The CSA relies on some approximations most likely to be satisfied in SAR systems with small bandwidth-to-center frequency ratios and small coherent integration angles. In addition these approximations result in a residual 2-D space-variant phase effect in the final image. The use of the space-invariant matched filters is also a primary limiting factor in the CSA performance. For SAR systems that employ chirps for transmitted pulses, chirp-type interferences caused by moving objects in the terrain should be removed if high-resolution imaging is to be achieved. These factors have been widely researched with the aim of improving the CSA's overall functionality and behavior. Yet, all the improvements or comparisons to the CSA to-date are FFT-based [6-8]. The most important parameter for the CSA is its inherent dependency on chirping which is used both in the transmission and reference signals thus benefiting from the great advantage of using the FrFT in detecting Linear Frequency Modulated (LFM) signals.

A new FrFT-based Chirp Scaling Algorithm, termed the "*Fractional Chirp Scaling Algorithm*", FrCSA is illustrated in Figure 2. This algorithm involves the development of a model for transformation optimization in order to obtain the proper rotation angle α (required for the received chirped signal and all reference signals used in the algorithm). The model shown in Figure 2 uses a Local Optimization Procedure (LOP) [9] that investigates all possible rotation angles and selects the optimum value which is stored and used throughout the algorithm. The new FrCSA replaces all the FFTs modules in the conventional CSA with FrFTs as illustrated in Figure 2.

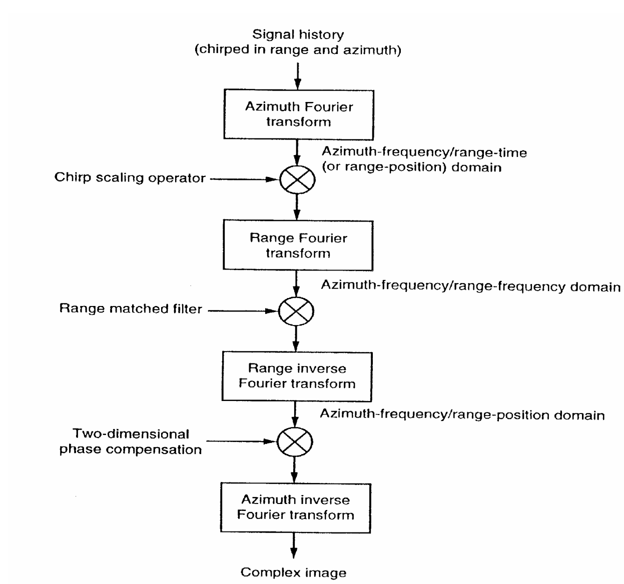

Fig. 1. FFT-based Chirp Scaling Algorithm [4]

One of the most important steps in the FrFT computation is in range transformation processing and its fractional correlator based range matched filter [10]. It is indeed this new module that gives the FrCSA its unique strength relative to the FFT-based CSA in handling signals particularly at the far end of the scene.

Table 1 illustrates the differences between the conventional CSA and the new FrCSA. The CSA relationships shown in table 1 are taken from [11]. The relationships for the FrCSA have been mathematically derived and the expressions are shown in table 1. These show the effect of using the FrFT in place of the classical FFT. The modification parameter, *D*, is scaled according to the optimum rotation requirements for the transform. The dependency of the two matched filter reference functions on the rotation angle results in optimal sidelobe reduction.

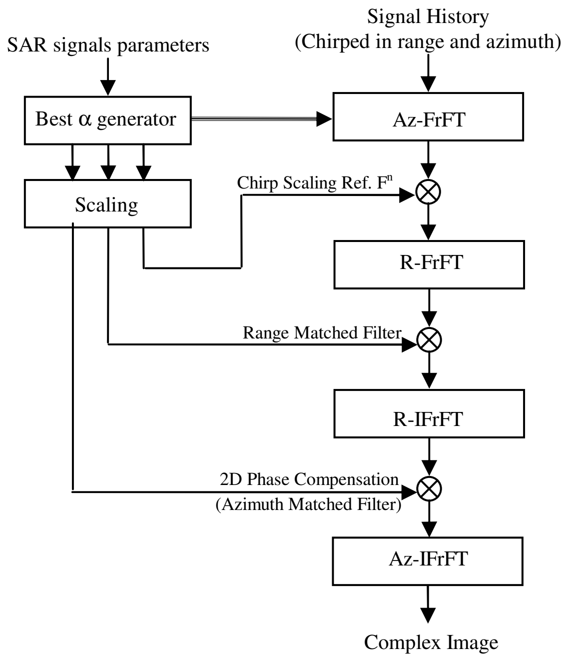

Fig. 2. FrFT-based Chirp Scaling Algorithm

4. RESULTS

The L-band SAR parameters from [11] were used to compare the differences in the constructed images from both of the conventional CSA and the new FrCSA. The computational cost of the FrCSA was approximately six times that of the CSA, as measured on a standard computer with 2.4 GHz speed and 512 MB RAM. This is because of the additional computational cost required for the transformation optimization module (best α generator) to detect the azimuth/range chirp rate of the signal being transformed and to produce the appropriate transformation order required for optimum azimuth/range-FrFT output response. Sample results for a unity power strength point target placed at the far range of the scene at position (135m, 138m, 0) are shown in figure 3 (zoomed). As the target is at the far range of the scene the complex returns exhibits severe range curvature resulting in difficulties obtaining the resolved processed target. Figure 3(a) is the contour plot of the CSA normalized complex image, and figure 3(b) is the contour plot of the FrCSA normalized complex image. From these images we note that the sidelobes of the FrCSA are much better suppressed than that of the CSA. The resolution of the point targets for the FrCSA is better than that of the CSA.

Optimum filtering in this fractional domain [10] is now used to extract the power spectrum density (PSD) plots of the CSA and the FrCSA producing Figure 4(a) and 4(b) respectively. It can be seen that relative to the classical FFT-based CSA, the new FrCSA delivers an enhanced Signal-to-Noise Ratio (SNR). Computing the simulated targets SNRs outputs for the FrCSA and CSA, a 14 dB increase in the SNR of the FrCSA over the CSA was achieved. Furthermore from Figure 4, it is observed that the FrCSA offers better focusing capabilities and greater Side Lobe Reduction Ratio (SLRR). Notice that all these benefits are obtained, without the need for any additional focusing or enhancement techniques (required in classical FFT-based CSAs [12-14]).

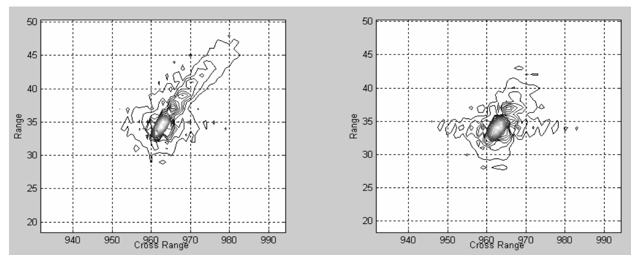

(a) (b)

Fig. 3. Point target at the far range of the scene window (zoomed) for (a) CSA and (b) FrCSA

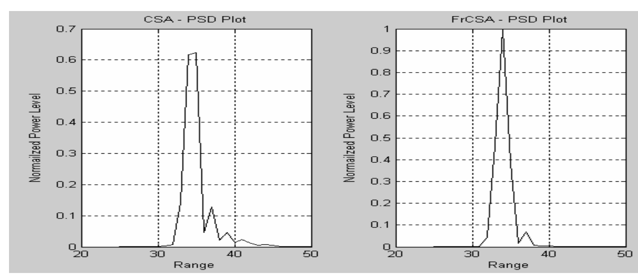

(a) (b)

Fig. 4. Normalized PSD comparison of (a) CSA and (b) FrCSA

TABLE 1 CSA / FRCSA PARAMETERS COMPARISON AND SYMBOLS

	CSA	FrCSA
Modification Parameter dependence	$D=\frac{1}{A_X}-1$	$D=\left[\frac{\csc\alpha}{A_x}-\frac{\cot\alpha}{b_m}\right]-1$
Range Matched Filter phase dependence	$\phi_A=-\frac{A_x\Delta K_R^2}{2b_m}$	$\phi_A=-\frac{1}{2}\left[\frac{A_x\csc\alpha}{b_m}-\cot\alpha\right]\Delta K_R^2$
Azimuth Matched Filter phase dependence	$\phi_C=\frac{b_m}{2}(1-A_x)(\frac{R_B}{A_x}-R_s)^2$	$\phi_C=\frac{b_m}{2}\left(1-\frac{A_x}{\csc\alpha}\right)\left(\frac{R_B}{A_x}-R_s\right)^2$

Symbol	Definition	Symbol	Definition
K_x	Frequency domain counterpart to the along-track direction	b_m	Generalized chirp rate
K_R	Instantaneous spatial transmitted frequency scaled by 2/c	ΔK_R	The variation in K_R over the transmitted bandwidth
K_{RC}	The value of K_R at the radar center frequency	R_s	Slant Range to scene center
A_x	$\sqrt{1-\frac{K_x^2}{K_{RC}^2}}$	R_B	Broadside target range
$D(Kx)$	Modification parameter	Y_s	Range position (the spatial equivalent to the fast time)
X_t	Target azimuth coordinate		

5. CONCLUSIONS

The *Wigner distribution* (WD) is one way of viewing the energy distribution of a signal in time-frequency domain. The FrFT rotates the WD in clockwise direction by an angle α in the time-frequency plane. In this way, the chirp signal is converted to a harmonic signal as there exists an optimum order of transformation for which the signal is compact. The method used for obtaining the optimum order of transformation is based on frame-by-frame process. In practice, the optimum parameter requires an efficient online procedure for its computation.

The Fractional Chirp Scaling Algorithm (FrCSA) has been applied for high resolution-high focused SAR imaging and initial results appear promising. The software implementation of the proposed algorithm, which is based on the continuous 1-D FrFT, was found to exhibit long processing times and large memory usage requirements. This can be overcome by hardware implementation using suitable parallel processors as in [15]. In addition, using a fast FrFT-code may be very useful in tackling this problem. However, the existence of efficiently and accurate digital fast FrFT code has not yet been developed [17]. In addition, the novel use of the 2-D Affine Generalized Fractional Fourier Transform (AGFFT) [18] in the FrCSA is under development. The proposed FrCSA in its basic form opens the field for a wide area of research that could result in the development of a new generation of high resolution – high focused SAR imaging algorithms.

6.REFERENCES

[1] L. Yu, W. Huang, M. Huang, Z. Zhu, X. Zeng, and W. Ji, "The Laguerre-Gaussian Series Representation of Two-Dimensional Fractional Transform," *Journal of Physics*, IOP Publishing Ltd, UK, pp. 9353-9357, 1998

[2] L. B. Almeida, "The Fractional Fourier Transform and Time-Frequency Representations," *IEEE Transactions on Signal Processing*, Vol. 42, No. 11, pp. 3084-3091, November 1994

[3] H. M. Ozaktas, Z. Zalevsky, and M. A. Kutay, "*The Fractional Fourier Transform: with Applications in Optics and Signal Processing,*" John Wiley & Sons Ltd, UK, January 2001

[4] R. K. Raney, H. Runge, R. Bamler, I. G. Cumming, and F. H. Wong, "Precision SAR Processing using Chirp Scaling," *IEEE Transaction on Geoscience and Remote Sensing*, Vol. 32, No. 4, pp. 786-799, July 1994

[5] A. S. Amein, and John. J. Soraghan, "A New Chirp Scaling Algorithm Based on the Fractional Fourier Transform," *IEEE Signal Processing Letters*, Vol. 12, No. 10. October 2005

[6] A. Moreira, J. Mittermayer, and R. Scheiber, "Extended Chirp Scaling Algorithm for Air-and Spaceborne SAR Data Processing in Stripmap and ScanSAR Imaging Modes," *IEEE Transactions on Geoscience and Remote Sensing*, Vol. 34, No. 5, pp. 1123-1136, September 1996

[7] J. Mittermayer, R. Lord, and E. Börner, "Sliding Spotlight SAR Processing for TerraSAR-X Using a New Formulation of The Extended Chirp Scaling Algorithm," *Proceedings of IGARSS2003*, IEEE, Vol. 3, pp. 1462-1464, France, July 2003

[8] A. Potsis, A. Reigber, A. Moreira, L. Ferro-Famil, and N. K. Uzunoglou, "Comparison of Chirp Scaling and Wave Number Domain Algorithms for Airborne Low Frequency SAR Data Processing," SAR Image Analysis, Modeling, and Techniques V, *SPIE Proceedings*, Vol. 4883, pp. 25-36, March 2002

[9] C. Capus, and K. Brown, "Short-Time Fractional Fourier Methods for the Time-Frequency Representation of Chirp Signals," *Journal of the Acoustical Society of America*, Vol. 113, No.6, pp. 3253-2363, June 2003

[10] D. Sazbon, Z. Zalevsky, E. Rivlin, and D. Mendlovic, "Using Fourier/Mellin-Based Correlators and their Fractional Versions in Navigation Tasks," *Journal of the Pattern Recognition Society*, ELSEVIER Science and Technology Ltd., Vol.35, pp. 2993-2999, 2002

[11] W. G. Carrara, R. S. Goodman, and R. M. Majewski, "*Spotlight Synthetic Aperture Radar: Signal Processing Algorithms,*" chapter 11, Artech House, Boston, London, 1994

[12] L. R. Varshney, and D. Thomas, "Sidelobe Reduction for Matched Filter Range Processing," *Proceedings of 2003 IEEE Radar Conference*, pp. 446-451, USA, May 2003

[13] A. Reigber, A. Potsis, E. Alivizatos, N. K. Uzunoglu, and A. Moreira, "Wavenumber Domain SAR Focusing with Integrated Motion Compensation," *Proceedings of IGARSS2003,* IEEE, pp. 4356-4358, France, July 2003

[14] D.W. Hawkins, and P. T. Gough, "An Accelerated Chirp Scaling Algorithm for Synthetic Aperture Imaging," *Proceeding of IGARSS97*, IEEE, pp. 471-473, Singapore, August 1997

[15] Y. Pi, H. Long, and S. Huang, "A SAR Parallel Processing Algorithm and its Implementation," *Proceedings of FIEOS2002 Conference*, USA, November 2002

[16] A. Bultheel, and H. E. Martínez Sulbaran, "Computation of the Fractional Fourier Transform," *Applied and Computational Harmonic Analysis*, Academic Press Inc., Vol. 16, No. 3, pp. 182-202, February 2004

[17] S.-C. Pei, J.-J. Ding, "Two-Dimensional Affine Generalized Fractional Fourier Transform," *IEEE Transactions on Signal Processing,* Vol. 49, No. 4, pp. 875-897, April 2001

[18] G. Franceschetti, R. Lanari, E.S. Marzouk, "A new Two-Dimensional Squint Mode SAR Processor," *IEEE Transaction on Aerospace and Electronic Systems*, Vol. 32, No. 2, pp. 854-863, April 1996.